

## Electronic Supplementary Information

for

### Photoinduced energy and electron transfer processes in a supramolecular system combining a tetrapyrrenylporphyrin derivative and arene-ruthenium metalla-prisms

Santiago Luis Pons Alles,<sup>a</sup> Daniele Veclani,<sup>b</sup> Andrea Barbieri,<sup>b</sup>

Bruno Therrien\*<sup>a</sup> and Barbara Ventura\*<sup>b</sup>

<sup>a</sup> *Institute of Chemistry, University of Neuchâtel, Avenue de Bellevaux 51, CH-2000 Neuchatel, Switzerland.*

<sup>b</sup> *Institute for Organic Synthesis and Photoreactivity (ISOF) – National Research Council (CNR), Via P. Gobetti 101, 40129 Bologna, Italy.*

#### Table of contents

<sup>1</sup> H and <sup>13</sup> C NMR spectra of <b>P-Pyr<sub>4</sub></b>	Pages S2
<sup>1</sup> H and DOSY NMR spectrum of <b>P-Pyr<sub>4</sub>@(Rucage)<sub>4</sub></b>	Page S3
HRMS-ESI spectrum of <b>P-Pyr<sub>4</sub></b> .	Page S4
Modified <b>Clip</b> used as a model for DFT calculations	Page S5
Electrochemical data for <b>Panel</b> and <b>Clip</b>	Page S5-S6
Additional absorption spectra	Page S6-S7
Additional emission and excitation spectra	Page S7-S8
Decay profiles for <b>P-Pyr<sub>4</sub>@(Rucage)<sub>4</sub></b>	Page S8
Transient absorption spectra of <b>Rucage</b> , <b>Clip</b> and <b>P-Pyr<sub>4</sub></b>	Pages S9-S10
Global analysis for <b>P-Pyr<sub>4</sub>@(Rucage)<sub>4</sub></b>	Page S10
Singlet oxygen phosphorescence	Page S11
Additional theoretical results	Pages S12-S20
Parameters for the energy transfer study	Pages S21-S24

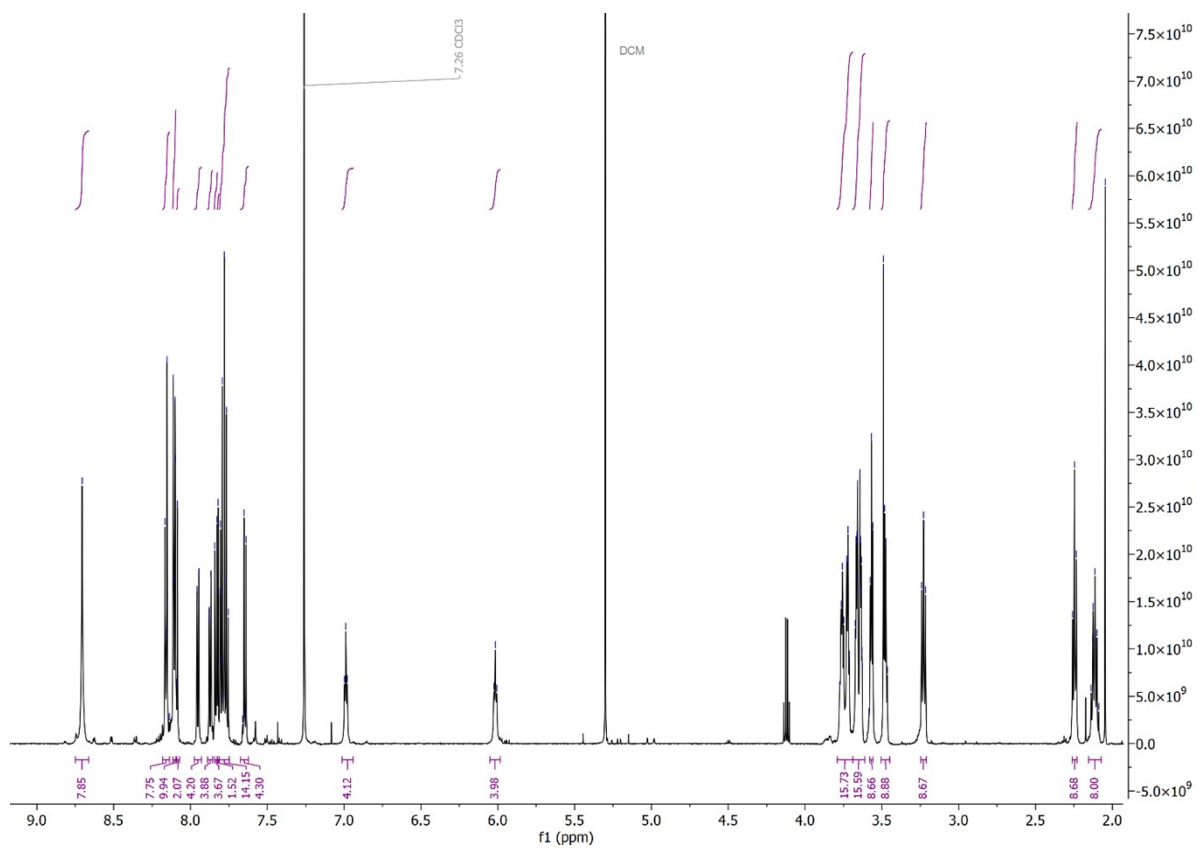


Figure S1. <sup>1</sup>H NMR spectrum of **P-Pyr<sub>4</sub>** (CDCl<sub>3</sub>).

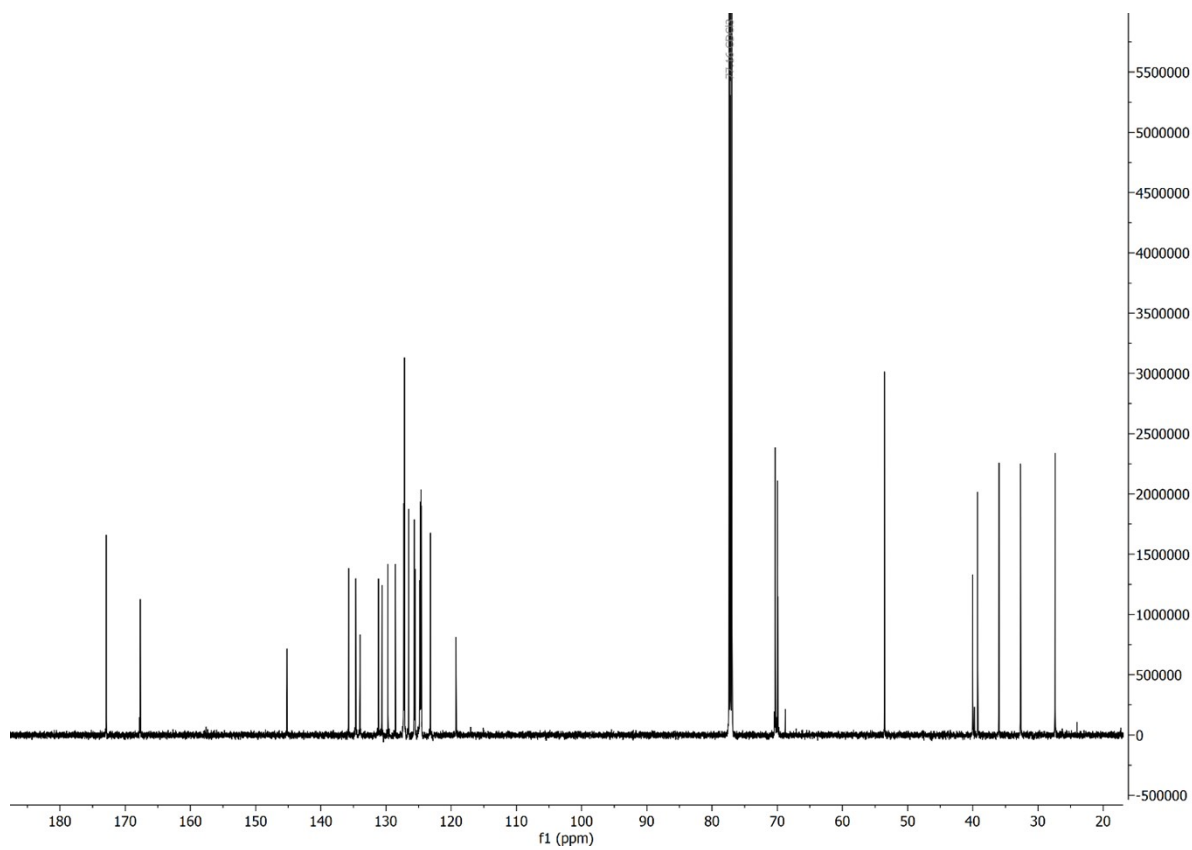


Figure S2. <sup>13</sup>C NMR spectrum of **P-Pyr<sub>4</sub>** (CDCl<sub>3</sub>).

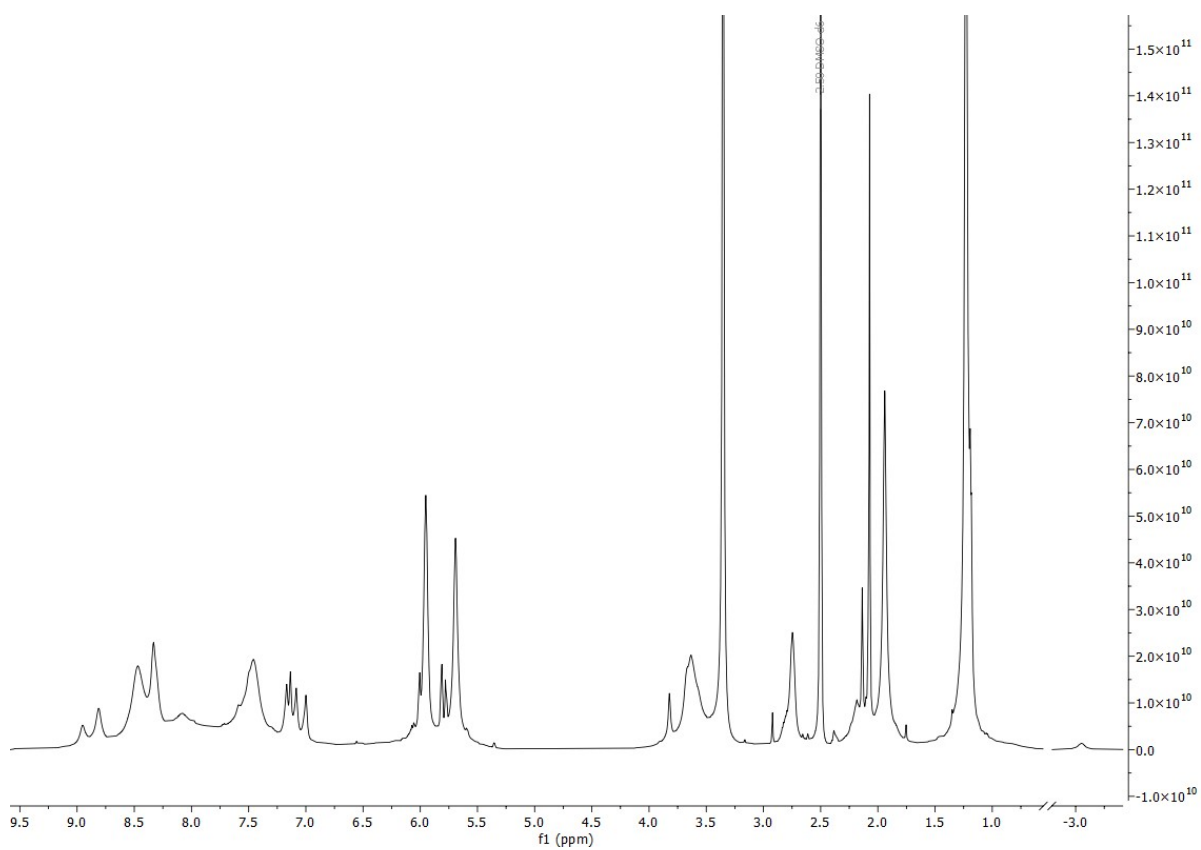


Figure S3.  $^1\text{H}$  NMR spectrum of **P-Pyr<sub>4</sub>@(Rucage)<sub>4</sub>** (DMSO).

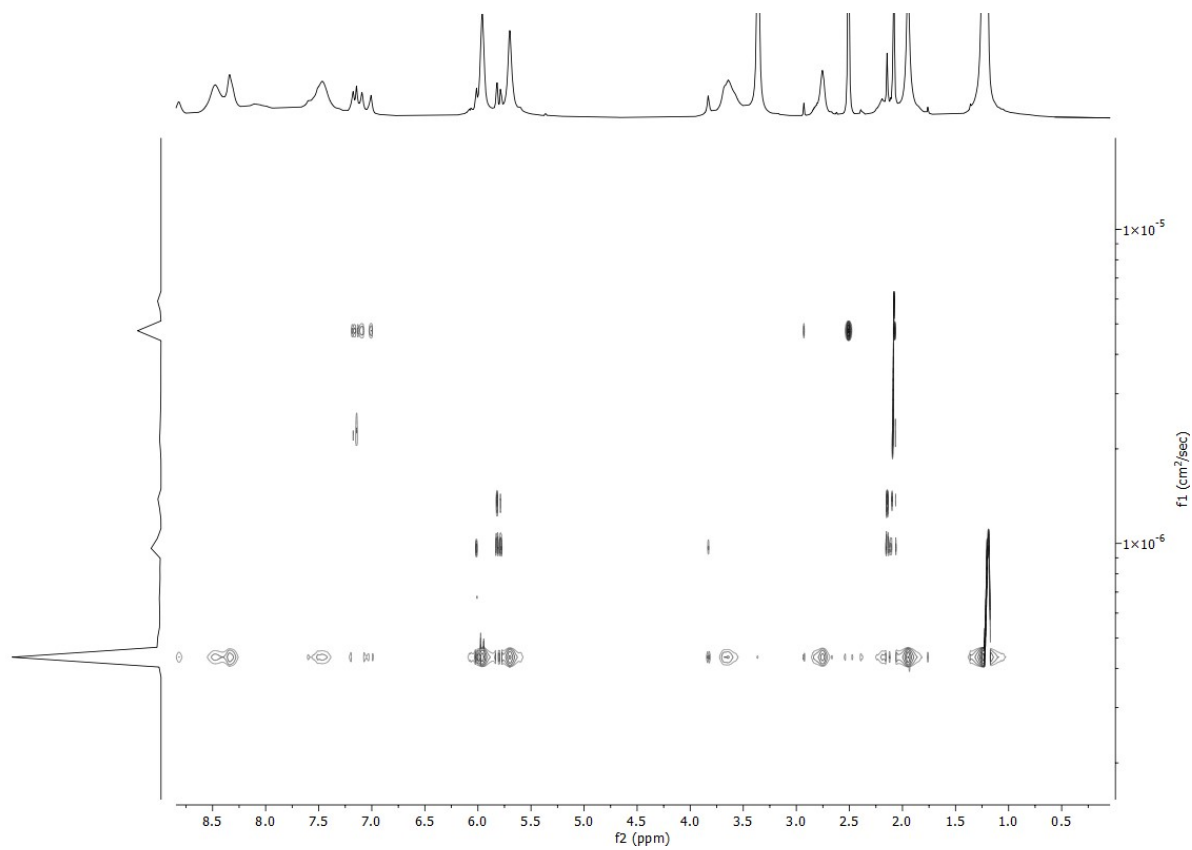


Figure S4. DOSY spectrum of **P-Pyr<sub>4</sub>@(Rucage)<sub>4</sub>** (DMSO).

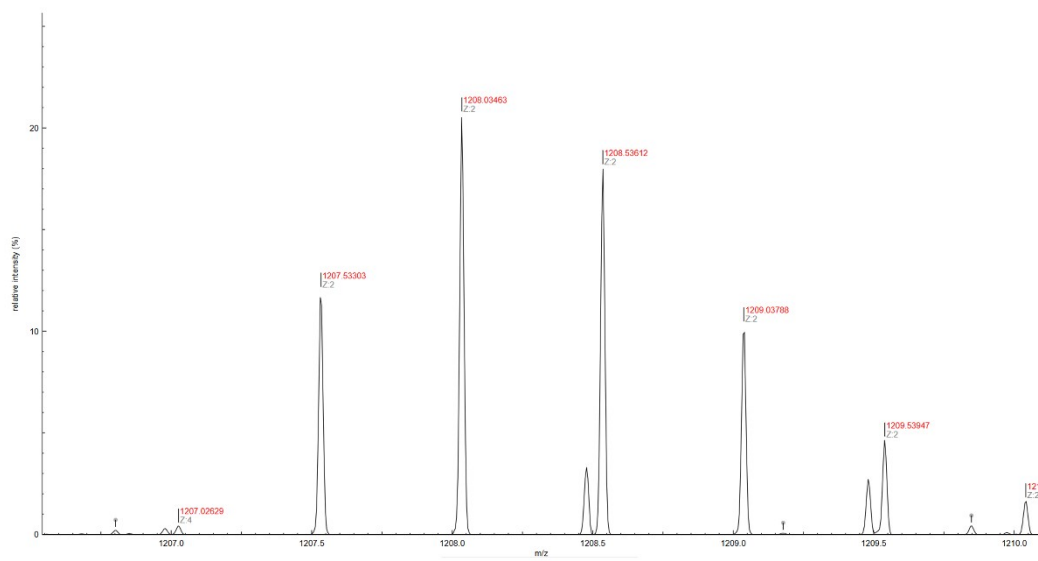
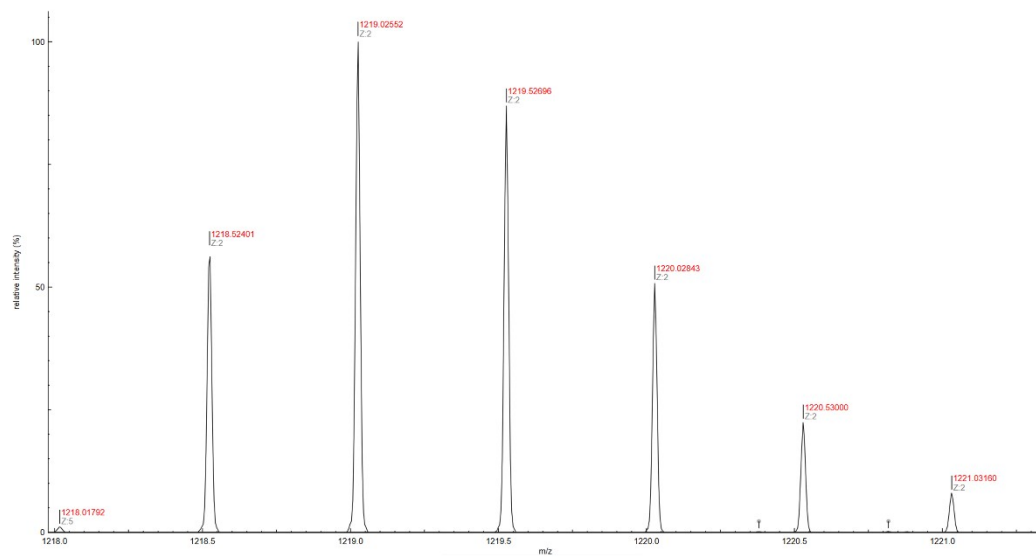
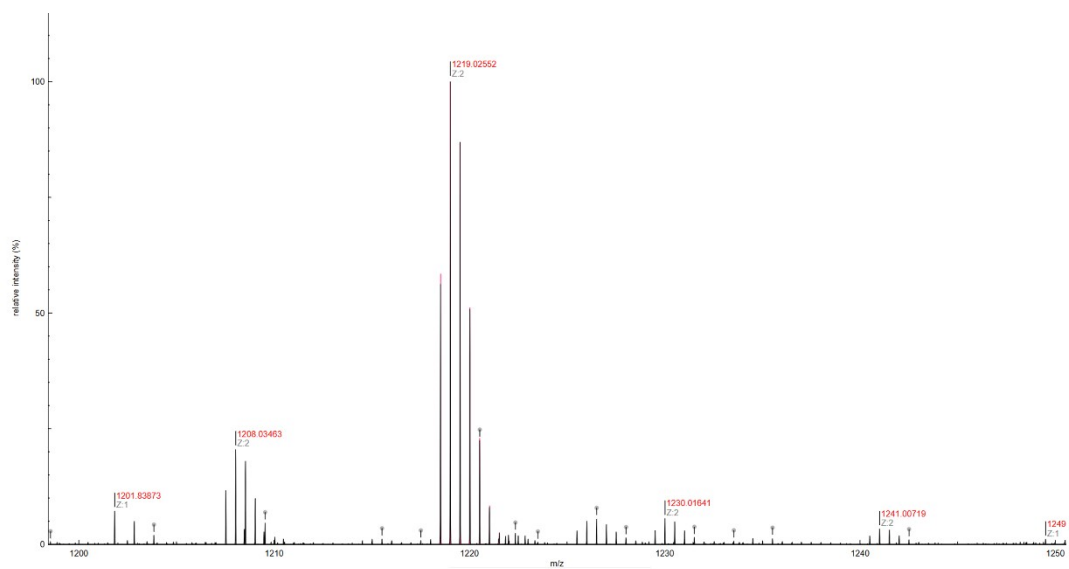


Figure S5. HRMS-ESI spectrum of P-Pyr<sub>4</sub>.

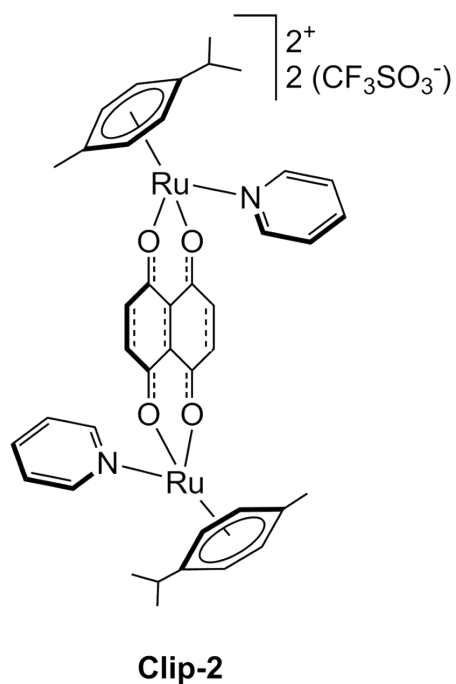


Figure S6. Modified **Clip** used as a model for DFT calculations.

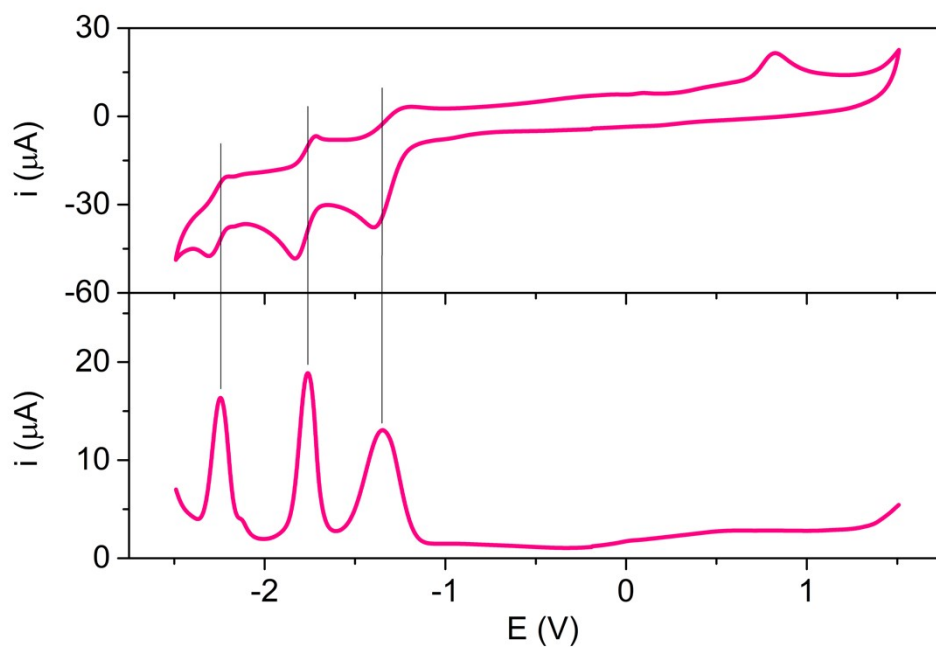


Figure S7. Cyclic (top panel) and square wave (bottom panel) voltammetry scans of **Panel** in DCM solution. CV cathodic scan starting from -0.2 V; SWV anodic and cathodic scans from -0.2 V (the sign of the cathodic current is reversed).

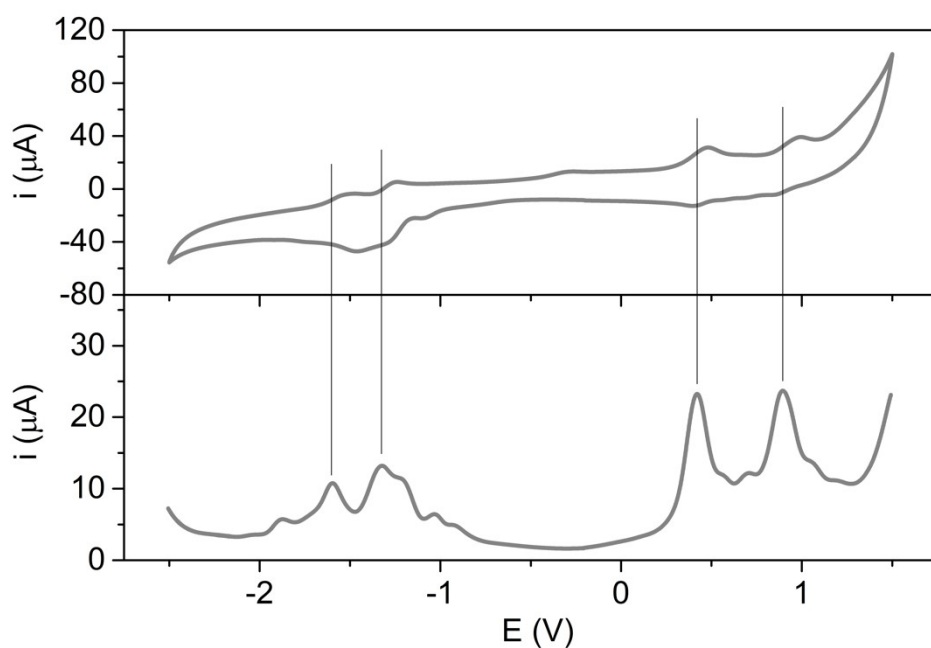


Figure S8. Cyclic (top panel) and square wave (bottom panel) voltammetry scans of **Clip** in DCM solution. CV cathodic scan starting from -0.2 V; SWV anodic and cathodic scans from -0.2 V (the sign of the cathodic current is reversed).

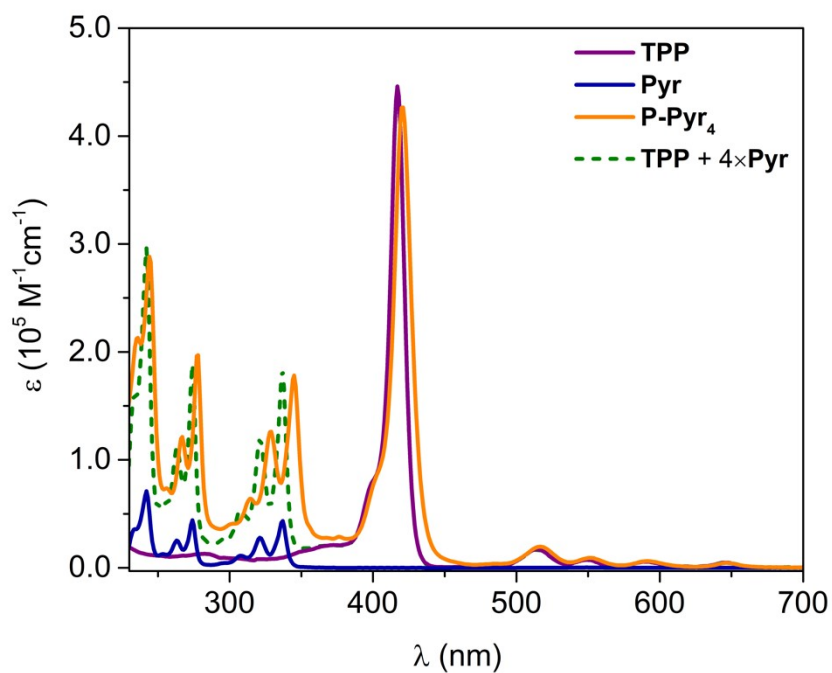


Figure S9. Absorption spectra of **P-Pyr<sub>4</sub>** and its respective models **TPP** and **Pyr** in DCM. The weighted sum of the spectra of the models is also reported.

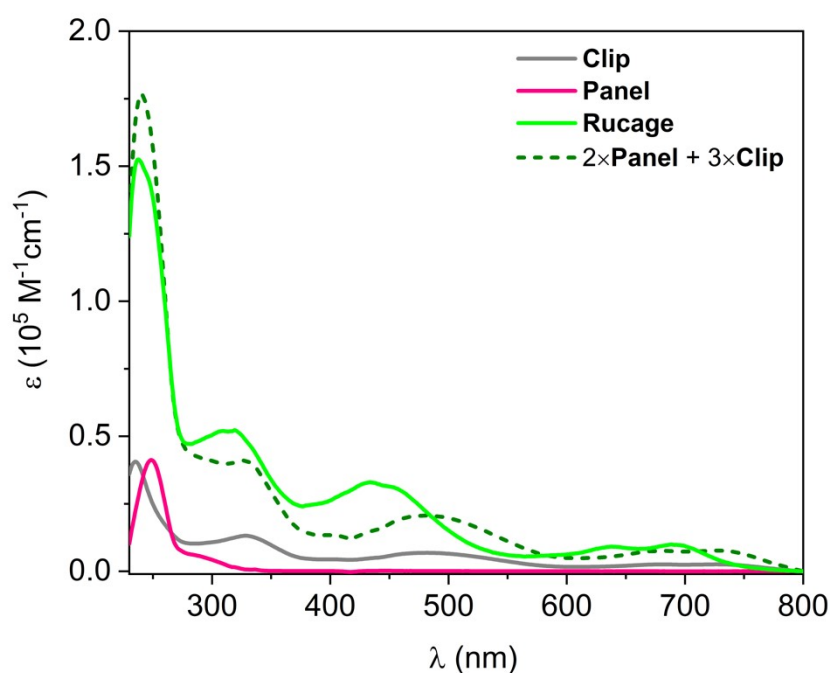


Figure S10. Absorption spectra of **Rucage** and its respective models **Clip** and **Panel** in DCM. The weighted sum of the spectra of the models is also reported.

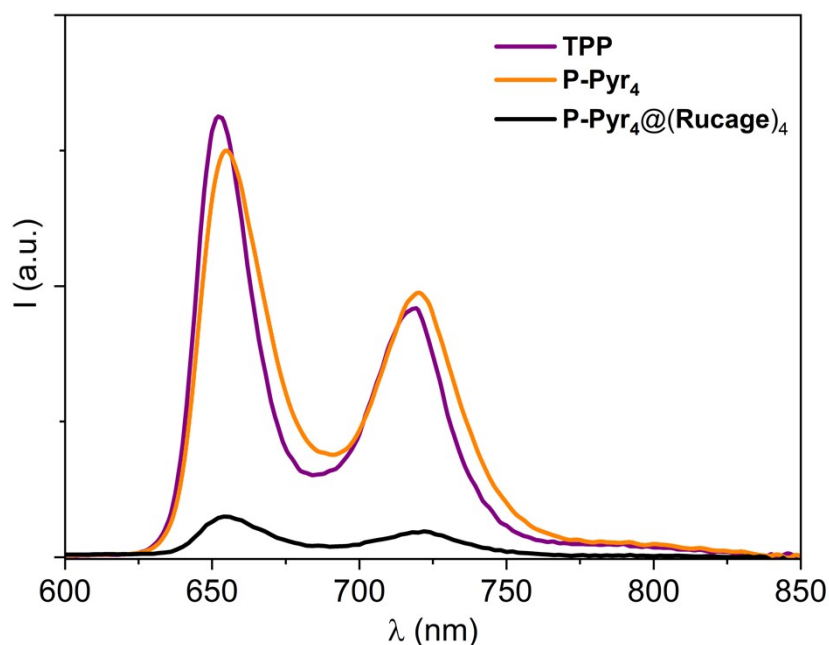


Figure S11. Corrected emission spectra of isoabsorbing solutions of **TPP**, **P-Pyr<sub>4</sub>**, and **P-Pyr<sub>4</sub>@(Rucage)<sub>4</sub>** in DCM; excitation at 515 nm ( $A_{515} = 0.13$ ). At this wavelength, 30% of the photons are absorbed by the porphyrins in the array, while the remaining 70% are absorbed by the Ru cages, so the measured intensities indicate that the porphyrin emission in **P-Pyr<sub>4</sub>@(Rucage)<sub>4</sub>** is quenched by a factor 3 with respect to the **TPP** model.

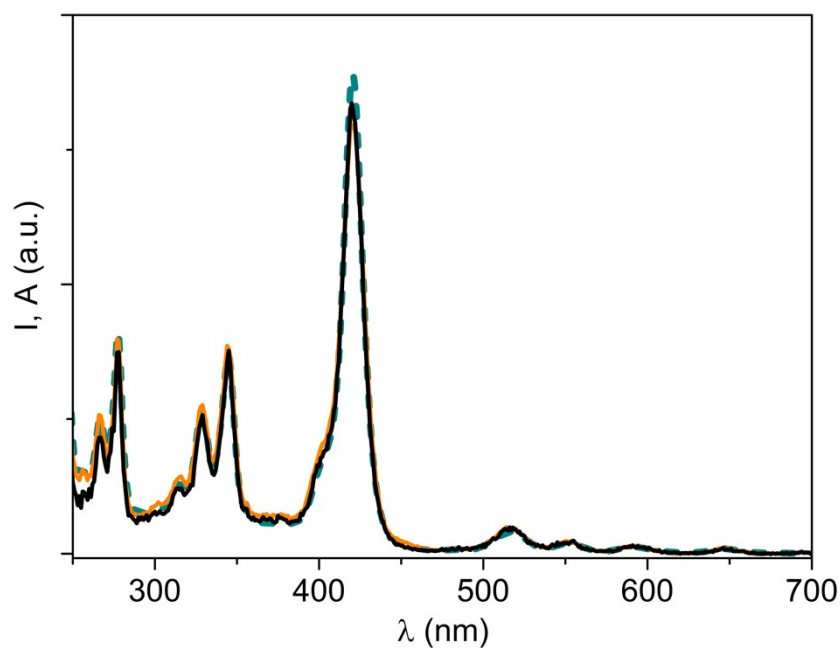


Figure S12. Arbitrarily scaled corrected excitation spectra of **P-Pyr<sub>4</sub>@(Rucage)<sub>4</sub>** (black) and **P-Pyr<sub>4</sub>** (orange) ( $\lambda_{em} = 720$  nm) and absorption spectrum of **P-Pyr<sub>4</sub>** (cyan dashed) in DCM.

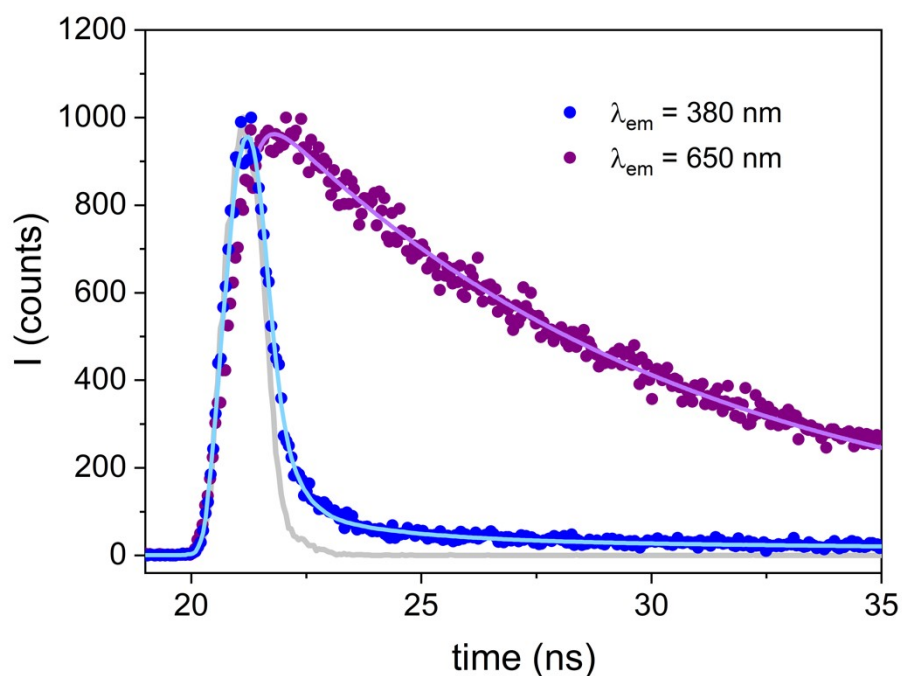


Figure S13. Decay profiles for **P-Pyr<sub>4</sub>@(Rucage)<sub>4</sub>**, measured with the single photon counting technique, upon excitation at 331 nm in DCM, at the indicated wavelengths. The lines represent the fittings (at 380 nm  $\tau = 360$  ps; at 650 nm  $\tau_1 = 350$  ps (rise),  $\tau_2 = 9.1$  ns). In grey is reported the prompt instrumental profile.

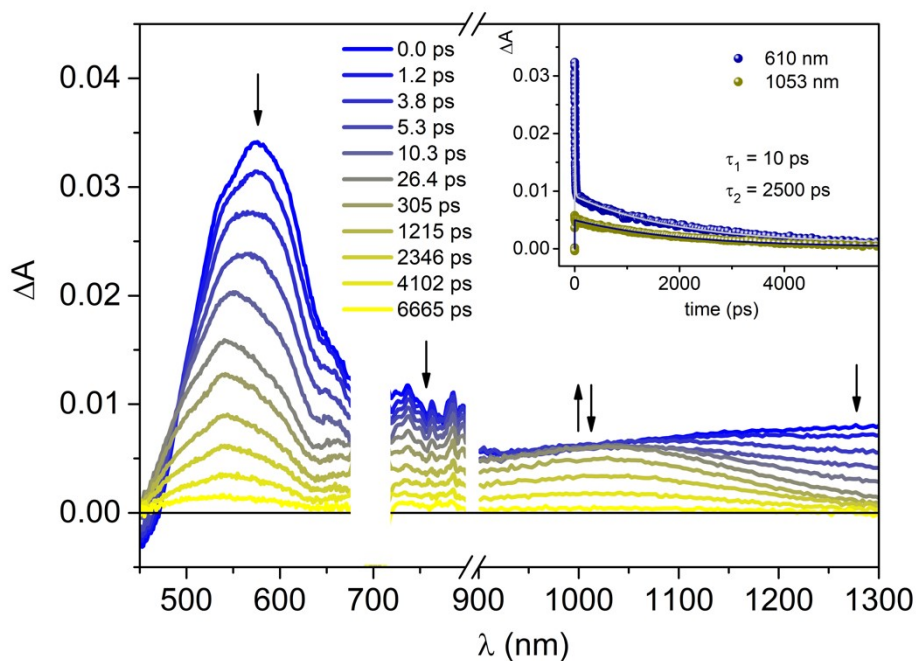


Figure S14. Transient absorption spectra of **Rucage** in DCM at different delays. Excitation at 700 nm ( $A_{700} = 0.34$ , 0.2 cm optical path, 10  $\mu\text{J}/\text{pulse}$ ). Inset:  $\Delta A$  time evolutions (dots) and fittings (lines) at the indicated wavelengths.

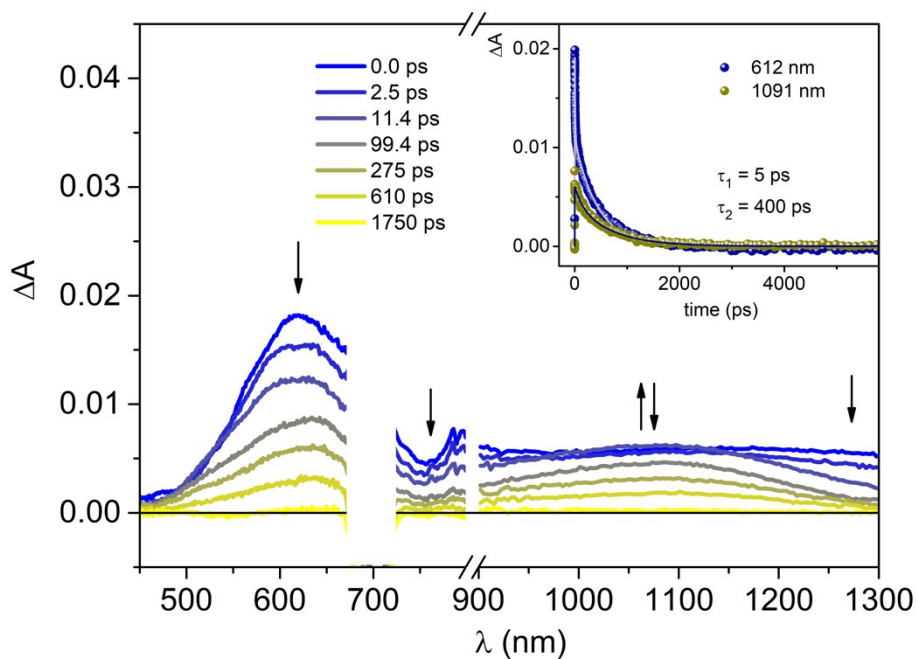


Figure S15. Transient absorption spectra of **Clip** in DCM at different delays. Excitation at 700 nm ( $A_{700} = 0.34$ , 0.2 cm optical path, 10  $\mu\text{J}/\text{pulse}$ ). Inset:  $\Delta A$  time evolutions (dots) and fittings (lines) at the indicated wavelengths.

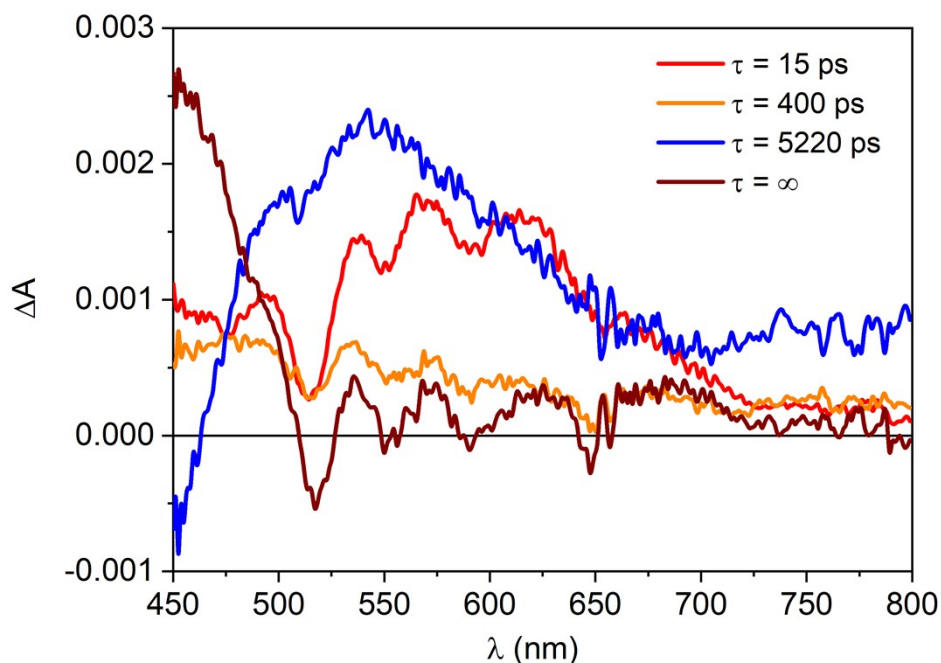


Figure S16. Spectral distribution of the amplitudes of the calculated lifetimes (indicated in the legend) from global fit analysis of the transient absorption matrix (obtained with four principal components and three expected lifetimes, with 400 ps as a fixed value, plus an infinite lifetime) of **P-Pyr<sub>4</sub>@(Rucage)<sub>4</sub>** in DCM.

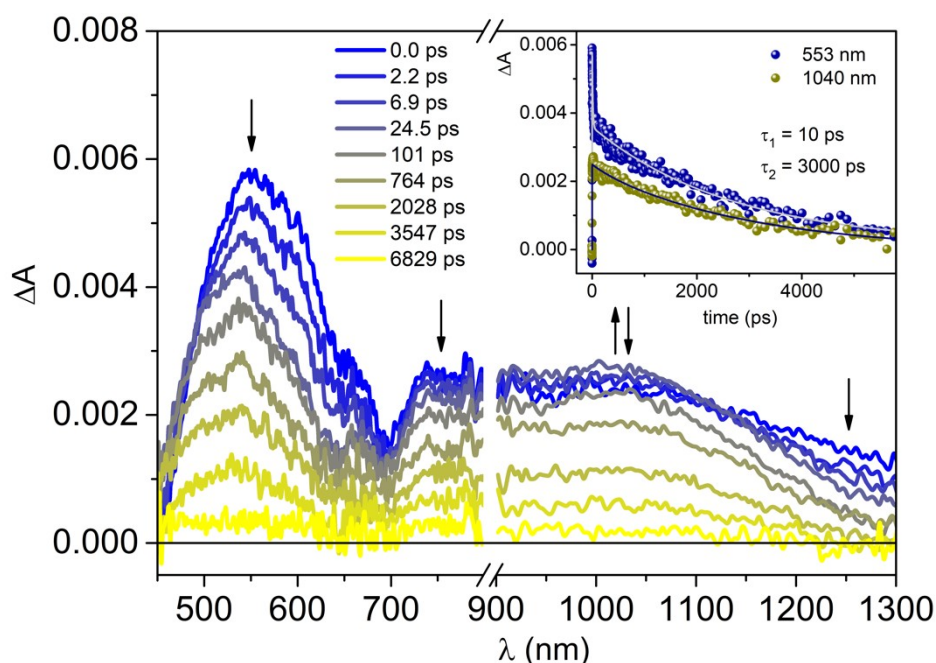


Figure S17. Transient absorption spectra of **Rucage** in DCM at different delays. Excitation at 420 nm ( $A_{420} = 0.24$ , 0.2 cm optical path, 1  $\mu\text{J}/\text{pulse}$ ). Inset:  $\Delta A$  time evolutions (dots) and fittings (lines) at the indicated wavelengths.

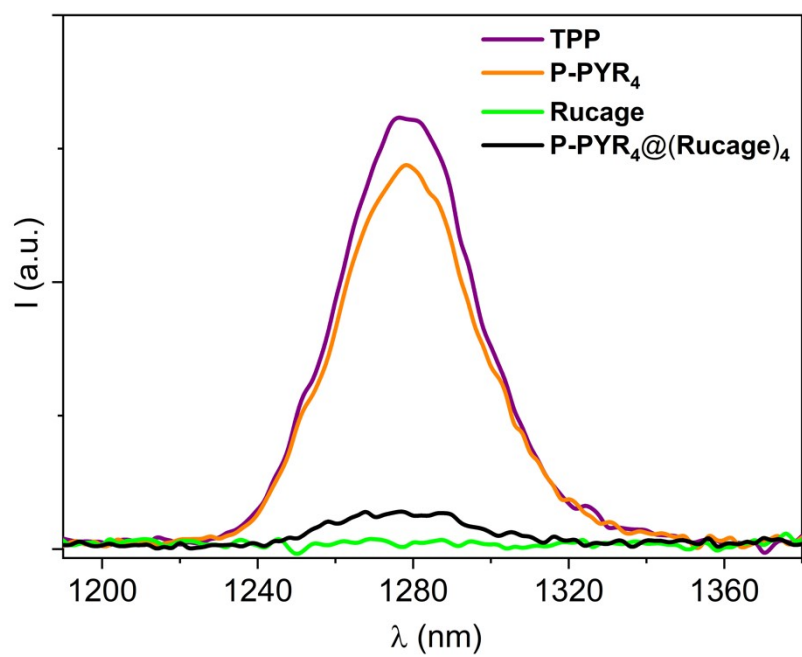


Figure S18. Singlet oxygen phosphorescence from optically matched solutions at 400 nm of **TPP**, **P-Pyr<sub>4</sub>**, **Rucage** and **P-Pyr<sub>4</sub>@(Rucage)<sub>4</sub>** in DCM ( $A_{400} = 0.3$ ).

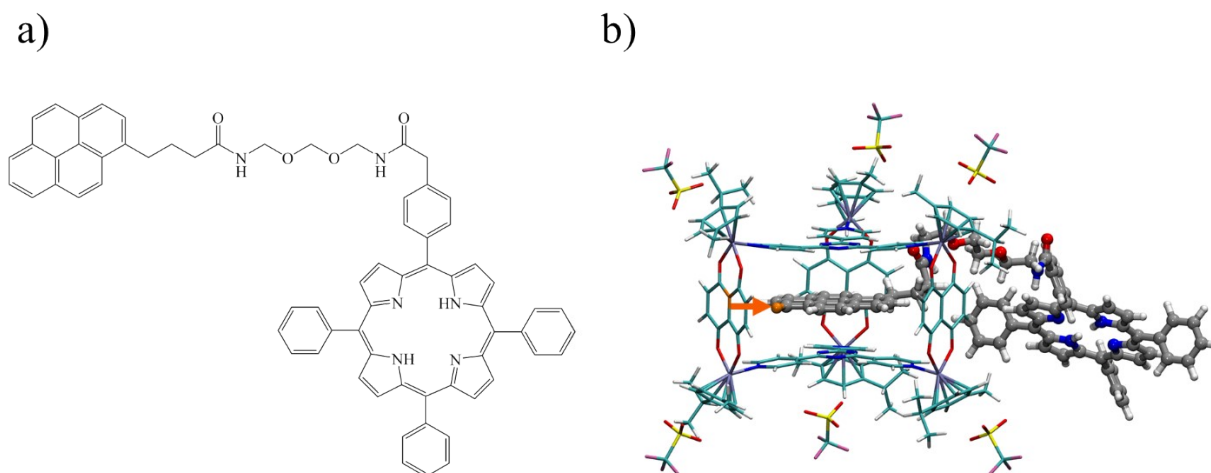


Figure S19. a) Schematic representation of **P-Pyr** model used for scan calculations; b) the optimized structure of **P-Pyr@Rucage** is the last point for scan calculation, the atoms involved in the scan are highlighted in orange with their relative scan direction. Scan started at a distance of 45.527 Å, where the two molecules no longer interact, up to 3.043 Å, a distance of minimum geometry. To facilitate the visualization of the two units, triflate anions are removed and the C atoms of **P-Pyr** (ball-and-stick model) are colored in silver, while those of **Rucage** (stick model) are reported in cyan.

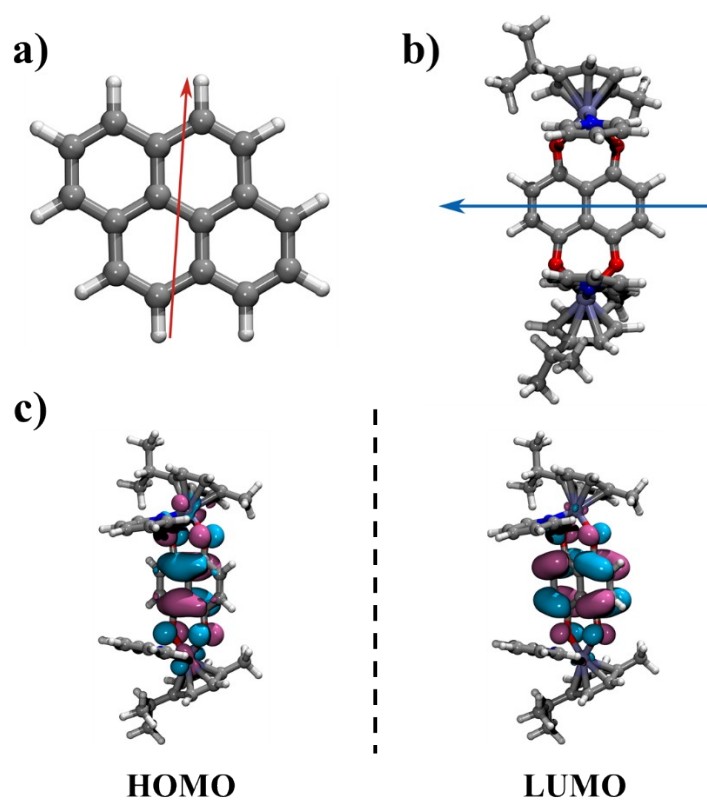


Figure S20. a) Electric dipole moment for **Pyr**; b) electric transition dipole moment between ground state and first excited states in modified **Clip-2**; c) HOMO and LUMO orbitals involved in the transitions.

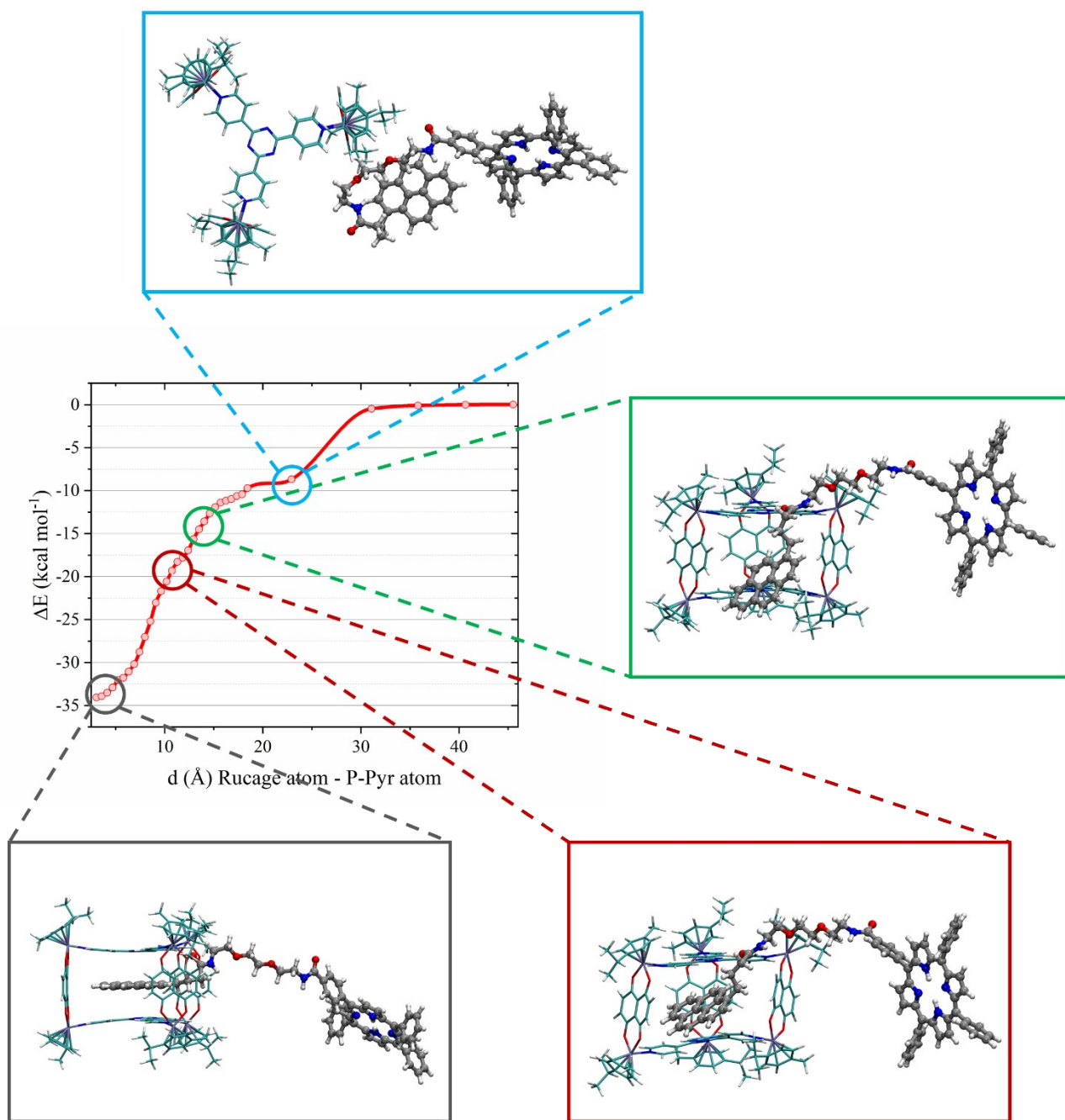


Figure S21. Scan calculations energy profile ( $\Delta E = E_{45\text{\AA}} - E_{X\text{\AA}}$ ;  $E_{45\text{\AA}}$  energy of last point;  $E_{X\text{\AA}}$  energy of the X point) with the most relevant structures obtained during the scan procedure. To facilitate the visualization of the two units, triflate anions are removed and the C atoms of **P-Pyr** (ball-and-stick model) are colored in silver, while those of **Rucage** (stick model) are reported in cyan.

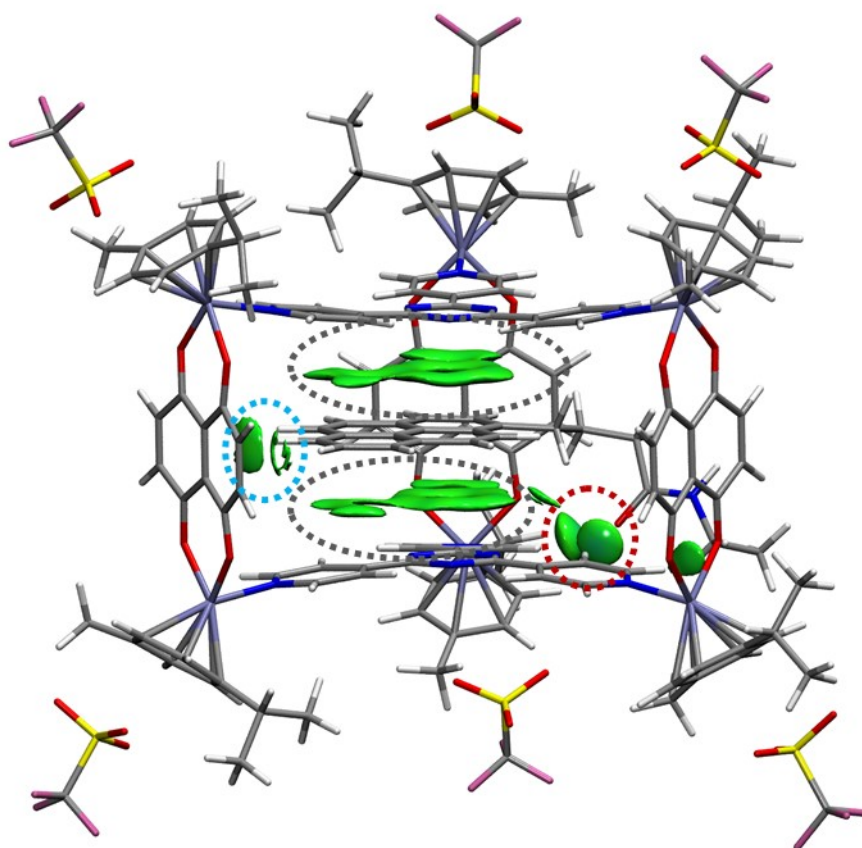


Figure S22. Minimum energy structures with the 3D IGM surfaces mapped using the product of the electron density and the second eigenvalue of the electron-density Hessian matrix. Green colored regions indicate non-covalent interactions:  $\pi$ - $\pi$  highlighted in grey, CH- $\pi$  highlighted in blue, and CH-O highlighted in red. The pegylated porphyrin moieties have been omitted for clarity.

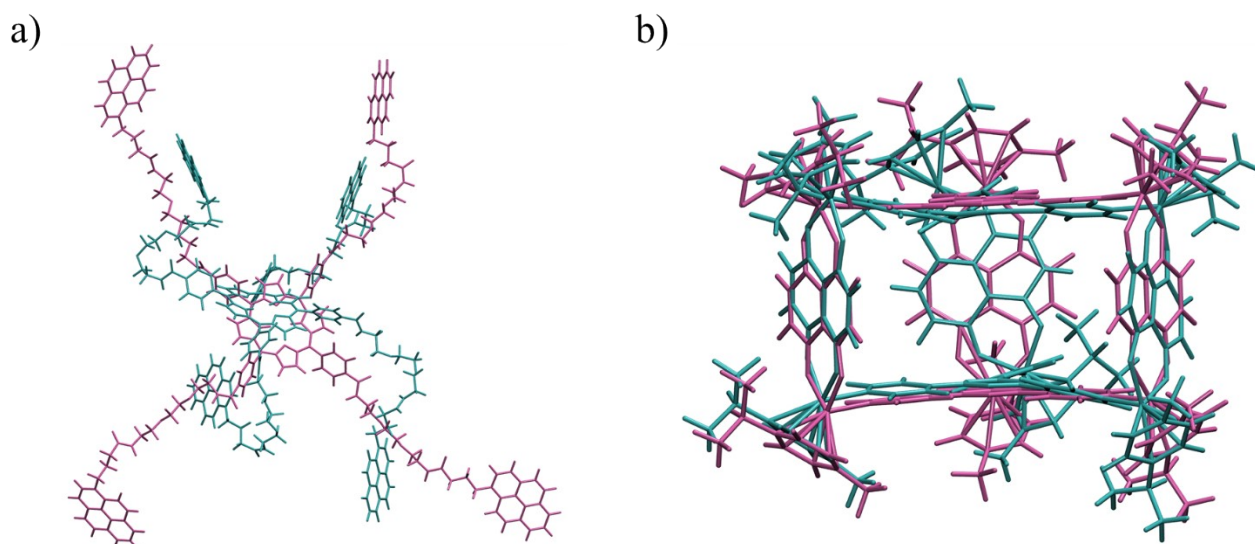


Figure S23. Overlap between optimized structures of: a) **P-Pyr<sub>4</sub>** and b) **Rucage** in **P-Pyr<sub>4</sub>@(Rucage)<sub>4</sub>\_VI** complex, where the *Def* is higher (cyan) and in the free system (purple).

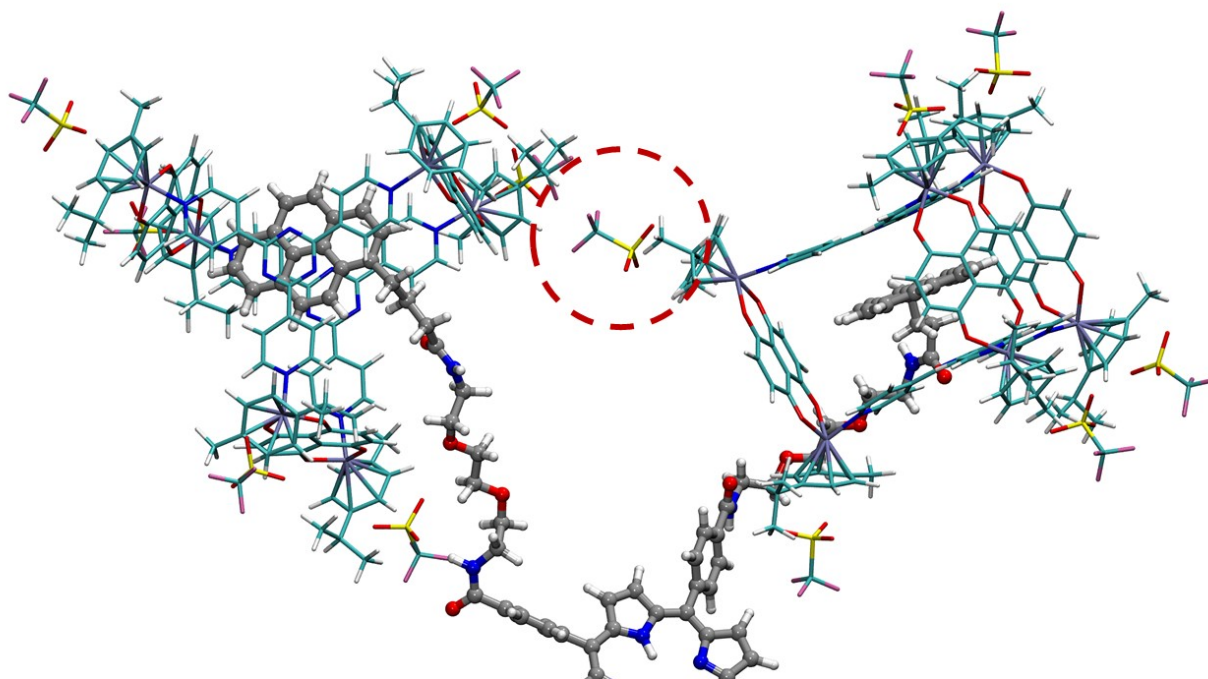


Figure S24. Detail of the optimized **P-Pyr<sub>4</sub>@(Rucage)<sub>4\_II</sub>** structure highlighting in red the **Rucage - Rucage** interaction involving a triflate anion.

Table S1. Decomposition of the  $|IE|$  to highlight the contribution of the encapsulation by a single **Rucage** to the total  $|IE|$  values for all conformers investigated, values (in kcal · mol<sup>-1</sup>) from the following equation:

$$IE = E_{E_{P-Pyr_4@Rucage-x}} - (E_{P-Pyr_4} + E_{Rucage-x})$$

where  $E_{P-Pyr_4@Rucage-x}$  is the energy of **P-Pyr<sub>4</sub>** and one single **Rucage**,  $E_{Rucage-x}$  is the energy of a single isolated cage at the coordinate of the complex, x indicates the number of the cage.

$ IE $ decompositions	<b>P-Pyr<sub>4</sub> + Rucage-1</b>	<b>P-Pyr<sub>4</sub> + Rucage-2</b>	<b>P-Pyr<sub>4</sub> + Rucage-3</b>	<b>P-Pyr<sub>4</sub> + Rucage-4</b>
<b>P-Pyr<sub>4</sub>@(Rucage)<sub>4_I</sub></b>	41.6	43.6	50.1	54.0
<b>P-Pyr<sub>4</sub>@(Rucage)<sub>4_II</sub></b>	47.5	43.6	56.4	54.9
<b>P-Pyr<sub>4</sub>@(Rucage)<sub>4_III</sub></b>	55.9	43.9	74.6	56.0
<b>P-Pyr<sub>4</sub>@(Rucage)<sub>4_IV</sub></b>	47.4	70.3	64.7	50.9
<b>P-Pyr<sub>4</sub>@(Rucage)<sub>4_V</sub></b>	50.3	68.7	64.5	50.6
<b>P-Pyr<sub>4</sub>@(Rucage)<sub>4_VI</sub></b>	52.9	74.0	69.8	72.9

Table S2. Decomposition of  $Def$  to highlight the contribution of a single fragment (**P-Pyr<sub>4</sub>** and **Rucage**) to the total  $Def$  for all conformers investigated, values (in kcal · mol<sup>-1</sup>) from the following equation:

$$Def_{Rucage} = E_{relax\_Rucage} - E_{Rucage}$$

<i>Def</i> decompositions	<b>P-Pyr<sub>4</sub></b>	<b>Rucage-1</b>	<b>Rucage-2</b>	<b>Rucage-3</b>	<b>Rucage-4</b>
<b>P-Pyr<sub>4</sub>@(Rucage)<sub>4</sub>_I</b>	5.8	1.9	2.7	2.7	1.4
<b>P-Pyr<sub>4</sub>@(Rucage)<sub>4</sub>_II</b>	10.5	2.4	0.9	1.6	1.8
<b>P-Pyr<sub>4</sub>@(Rucage)<sub>4</sub>_III</b>	9.7	5.2	1.3	6.6	4.7
<b>P-Pyr<sub>4</sub>@(Rucage)<sub>4</sub>_IV</b>	13.6	2.6	8.1	1.3	3.0
<b>P-Pyr<sub>4</sub>@(Rucage)<sub>4</sub>_V</b>	11.9	4.3	11.8	1.9	2.7
<b>P-Pyr<sub>4</sub>@(Rucage)<sub>4</sub>_VI</b>	10.2	8.6	15.6	9.3	7.44

Table S3. Interchromophoric donor-to-acceptor distances (**Pyr–Porph**) in Å.<sup>a</sup>

	I	II	III	IV	V	VI
<b>Porph-Pyr<sub>1</sub></b>	26.748	20.749	14.788	14.160	13.582	13.081
<b>Porph-Pyr<sub>2</sub></b>	26.922	23.968	24.139	11.004	11.801	10.382
<b>Porph-Pyr<sub>3</sub></b>	22.792	25.066	22.627	26.298	21.188	20.081
<b>Porph-Pyr<sub>4</sub></b>	23.803	25.618	21.591	27.231	24.019	17.334

<sup>a</sup> Distances between the center of the N<sub>4</sub> porphyrin ring (**Porph**) and the center of the pyrene moieties (**Pyr<sub>n</sub>**) in the **P-Pyr<sub>4</sub>@(Rucage)<sub>4</sub>** system (see Figure S25), calculated from the molecular modeling for the conformations I–VI; average distance  $d = 20.4 \pm 5.6$  Å.

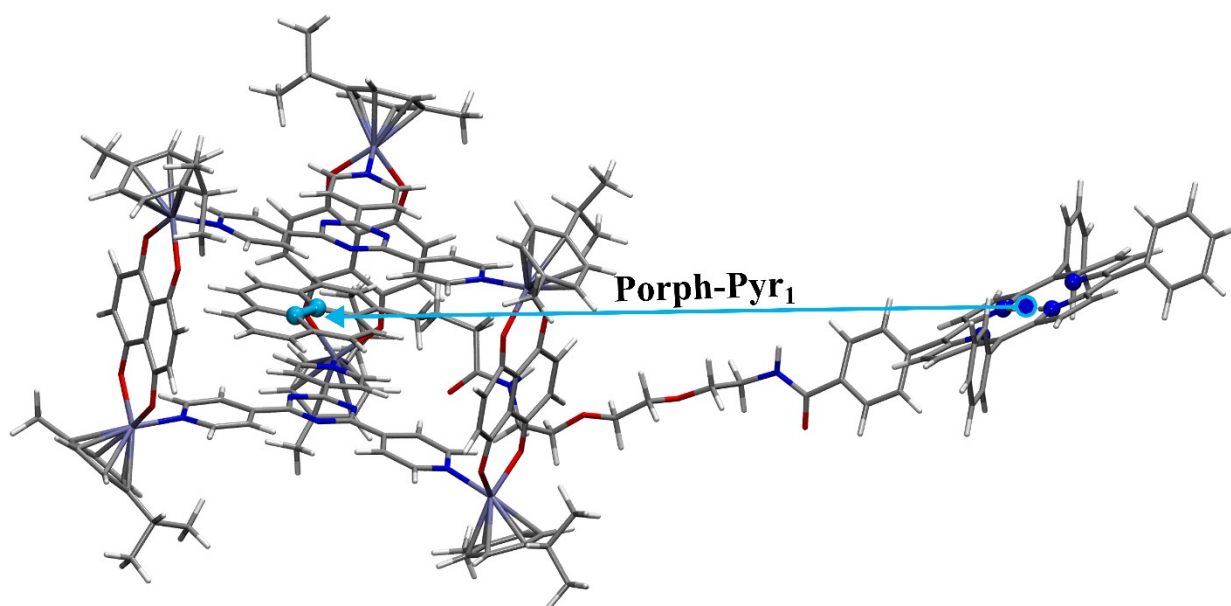


Figure S25. Sketch of the calculated interchromophoric distances **Porph-Pyr<sub>n</sub>**; as sake of clarity, only one over four arms of the porphyrin centre is shown.

Table S4. Interchromophoric donor-to-acceptor distances (**Pyr-Rucage**) in Å.<sup>a</sup>

	I	II	III	IV	V	VI
<b>Pyr<sub>1</sub>-Ruc<sub>1</sub></b>	7.321	6.878	8.660	9.030	6.712	6.736
<b>Pyr<sub>1</sub>-Ruc<sub>2</sub></b>	7.083	7.368	6.925	6.955	7.967	7.492
<b>Pyr<sub>1</sub>-Ruc<sub>3</sub></b>	8.744	8.906	7.178	7.142	8.631	8.631
<b>Pyr<sub>2</sub>-Ruc<sub>1</sub>'</b>	6.766	8.207	7.543	7.108	6.554	7.331
<b>Pyr<sub>2</sub>-Ruc<sub>2</sub>'</b>	8.974	8.517	6.710	8.904	6.816	8.872
<b>Pyr<sub>2</sub>-Ruc<sub>3</sub>'</b>	7.349	7.140	8.868	7.013	8.756	6.659
<b>Pyr<sub>3</sub>-Ruc<sub>1</sub>''</b>	6.777	7.020	8.312	7.832	7.107	6.975
<b>Pyr<sub>3</sub>-Ruc<sub>2</sub>''</b>	8.967	8.529	8.120	8.612	8.790	7.670
<b>Pyr<sub>3</sub>-Ruc<sub>3</sub>''</b>	6.501	7.483	6.407	6.776	7.045	8.081
<b>Pyr<sub>4</sub>-Ruc<sub>1</sub>'''</b>	6.848	7.298	8.956	7.477	6.747	8.971
<b>Pyr<sub>4</sub>-Ruc<sub>2</sub>'''</b>	9.075	8.331	7.336	6.798	8.862	6.796
<b>Pyr<sub>4</sub>-Ruc<sub>3</sub>'''</b>	7.218	7.203	6.846	8.800	7.483	7.542

<sup>a</sup>Distances between the center of the pyrene moieties (**Pyr<sub>n</sub>**) and the center of the naphthoquinonato pillars (**Ruc<sub>n</sub>**) in the **P-Pyr<sub>4</sub>@(Rucage)<sub>4</sub>** system (see Figure S26), calculated from the molecular modeling for the conformations I–VI; average distance  $d = 7.7 \pm 0.8$  Å.

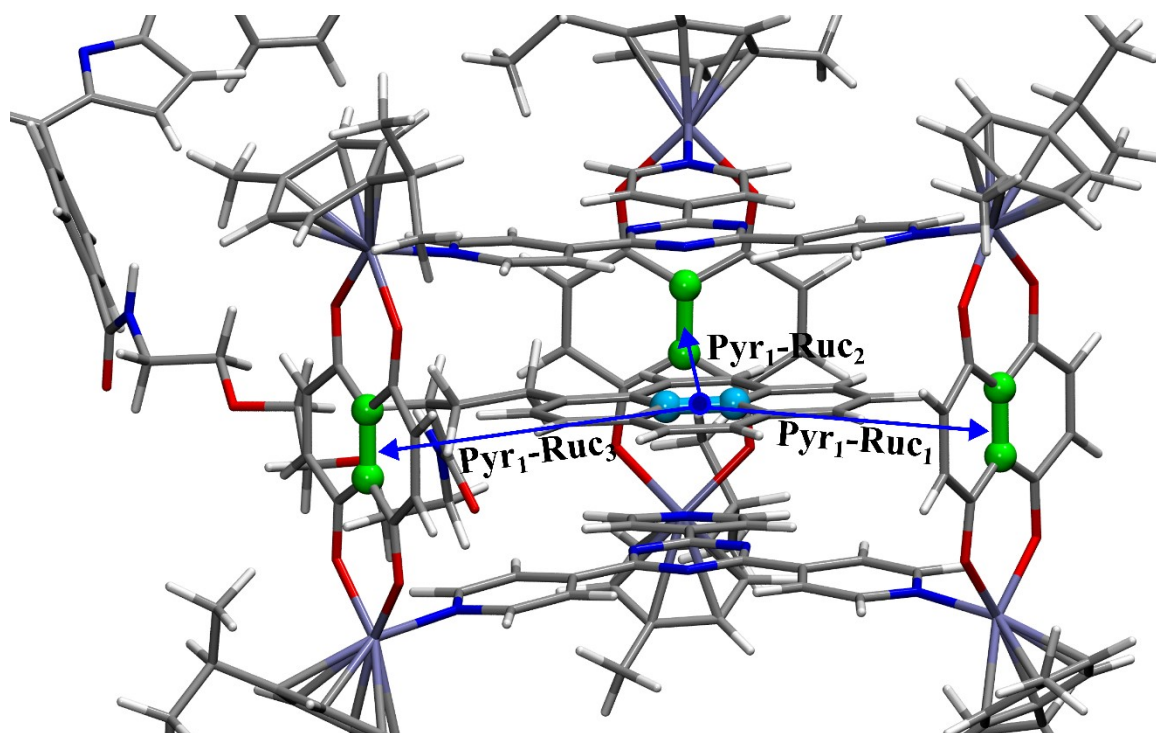


Figure S26. Sketch of the calculated interchromophoric distances **Pyr<sub>n</sub>-Ruc<sub>n</sub>**; as sake of clarity, only one over four arms of the porphyrin centre is shown.

Table S5. Interchromophoric donor-to-acceptor distances (**Porph-Rucage**) in Å.<sup>a</sup>

	I	II	III	IV	V	VI
<b>Porph-Ruc<sub>1</sub></b>	25.968	14.989	5.740	4.986	5.473	5.353
<b>Porph-Ruc<sub>2</sub></b>	19.338	24.186	15.212	15.354	16.720	16.566
<b>Porph-Ruc<sub>3</sub></b>	27.792	25.845	18.323	18.060	18.144	18.658
<b>Porph-Ruc<sub>1</sub>'</b>	15.192	19.646	17.451	5.456	5.086	4.793
<b>Porph-Ruc<sub>2</sub>'</b>	23.050	23.801	29.079	18.172	18.136	17.583
<b>Porph-Ruc<sub>3</sub>'</b>	28.173	29.894	25.068	16.894	15.347	13.670
<b>Porph-Ruc<sub>1</sub>''</b>	20.967	19.139	16.601	19.942	20.129	13.552
<b>Porph-Ruc<sub>2</sub>''</b>	30.728	24.492	24.215	27.037	13.124	12.720
<b>Porph-Ruc<sub>3</sub>''</b>	26.023	31.622	25.615	33.019	30.214	23.738
<b>Porph-Ruc<sub>1</sub>'''</b>	25.588	18.287	15.759	18.976	20.394	17.639
<b>Porph-Ruc<sub>2</sub>'''</b>	21.734	31.436	23.982	26.821	27.319	16.219
<b>Porph-Ruc<sub>3</sub>'''</b>	31.671	25.863	26.760	29.578	30.199	16.219

<sup>a</sup>Distances between the center of the N4 porphyrin ring (**Porph**) and the center of the naphthoquinonato pillars (**Ruc<sub>n</sub>**) in the **P-Pyr<sub>4</sub>@(Rucage)<sub>4</sub>** system (see Figure S27), calculated from the molecular modeling for the conformations I–VI; average distance  $d = 20.3 \pm 7.3$  Å.

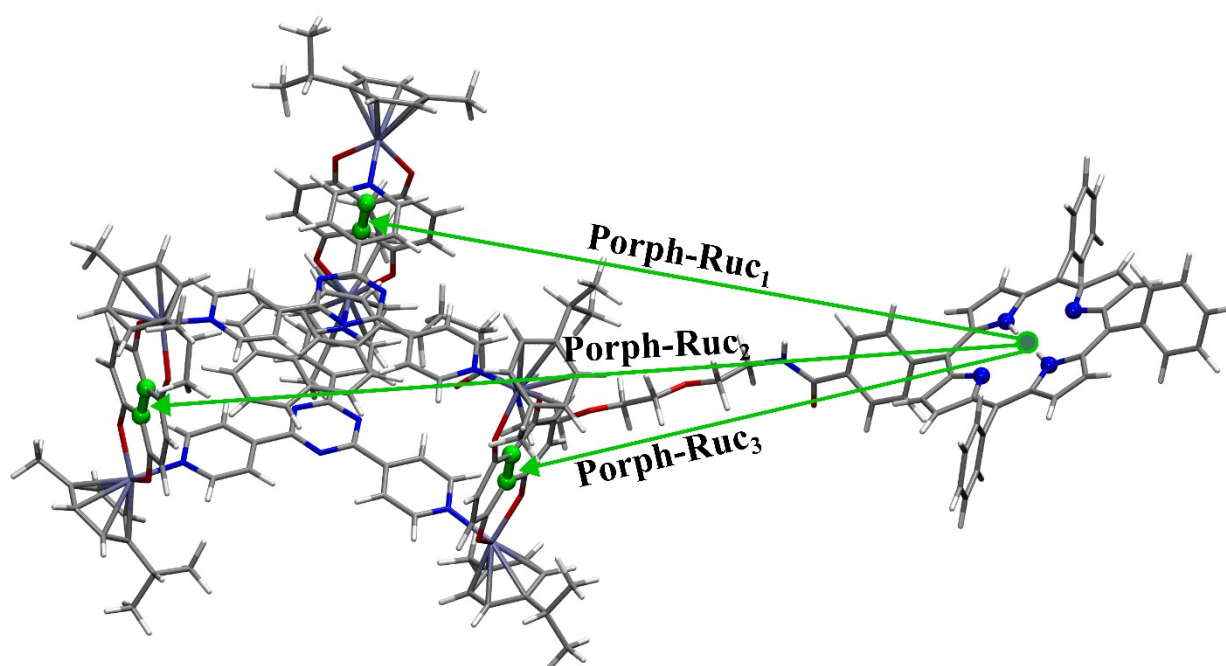


Figure S27. Sketch of the calculated interchromophoric distances **Porph-Ruc<sub>n</sub>**; as sake of clarity, only one over four arms of the porphyrin centre is shown.

Table S6. **Porph–Ru** distances (Å) in the different conformers (I–VI).<sup>a</sup>

	I	II	III	IV	V	VI
<b>Porph-Ru<sub>1</sub></b>	14.896	16.553	6.047	6.752	6.772	6.132
<b>Porph-Ru<sub>2</sub></b>	17.181	22.298	8.131	6.417	6.738	6.738
<b>Porph-Ru<sub>3</sub></b>	27.861	21.698	15.509	15.979	16.237	14.681
<b>Porph-Ru<sub>4</sub></b>	29.119	25.739	15.985	15.603	15.555	14.468
<b>Porph-Ru<sub>5</sub></b>	22.983	27.949	18.514	18.440	18.571	17.946
<b>Porph-Ru<sub>6</sub></b>	23.986	31.536	19.158	18.307	18.581	18.117
<b>Porph-Ru<sub>1</sub>'</b>	16.210	12.563	15.057	5.036	5.077	5.154
<b>Porph-Ru<sub>2</sub>'</b>	23.945	17.394	19.813	8.937	8.942	8.751
<b>Porph-Ru<sub>3</sub>'</b>	23.506	22.450	23.811	16.717	17.461	17.259
<b>Porph-Ru<sub>4</sub>'</b>	29.675	25.738	26.381	18.166	16.516	20.128
<b>Porph-Ru<sub>5</sub>'</b>	25.469	24.732	27.593	17.782	19.611	17.077
<b>Porph-Ru<sub>6</sub>'</b>	31.256	27.077	30.350	19.672	17.889	16.912
<b>Porph-Ru<sub>1</sub>''</b>	19.239	17.251	13.770	18.554	16.708	14.981
<b>Porph-Ru<sub>2</sub>''</b>	25.677	20.688	21.058	20.642	22.716	21.478
<b>Porph-Ru<sub>3</sub>''</b>	22.972	26.625	23.766	25.875	16.226	16.162
<b>Porph-Ru<sub>4</sub>''</b>	29.547	25.537	28.608	25.718	19.865	19.363
<b>Porph-Ru<sub>5</sub>''</b>	28.855	32.426	22.338	31.684	25.134	27.813
<b>Porph-Ru<sub>6</sub>''</b>	33.756	30.389	27.339	32.491	28.294	24.814
<b>Porph-Ru<sub>1</sub>'''</b>	18.431	20.272	13.231	16.614	15.249	12.843
<b>Porph-Ru<sub>2</sub>'''</b>	25.045	18.768	19.885	22.876	22.415	12.141
<b>Porph-Ru<sub>3</sub>'''</b>	24.087	25.370	24.299	25.115	23.872	23.270
<b>Porph-Ru<sub>4</sub>'''</b>	29.202	24.006	28.716	29.680	28.917	23.431
<b>Porph-Ru<sub>5</sub>'''</b>	28.975	32.169	22.248	27.887	25.365	15.943
<b>Porph-Ru<sub>6</sub>'''</b>	33.495	31.157	26.847	32.207	30.452	15.460

<sup>a</sup>Distances between the center of the N<sub>4</sub> porphyrin ring (**Porph**) and the ruthenium atoms (**Ru<sub>n</sub>**) in the **P-Pyr<sub>4</sub>@(Ru cage)<sub>4</sub>** system (see Figure S28), calculated from the molecular modeling for the conformations I–VI; average distance  $d = 20.8 \pm 7.0$  Å.

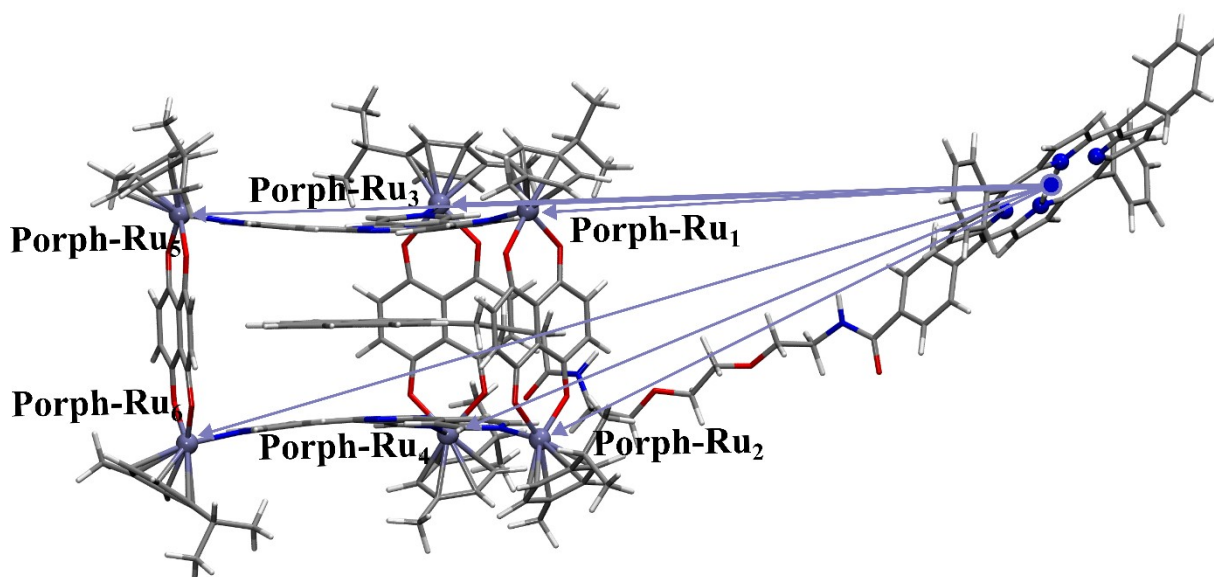


Figure S28. Sketch of the calculated interchromophoric distances **Porph-Ru<sub>n</sub>**; as sake of clarity, only one over four arms of the porphyrin centre is shown.

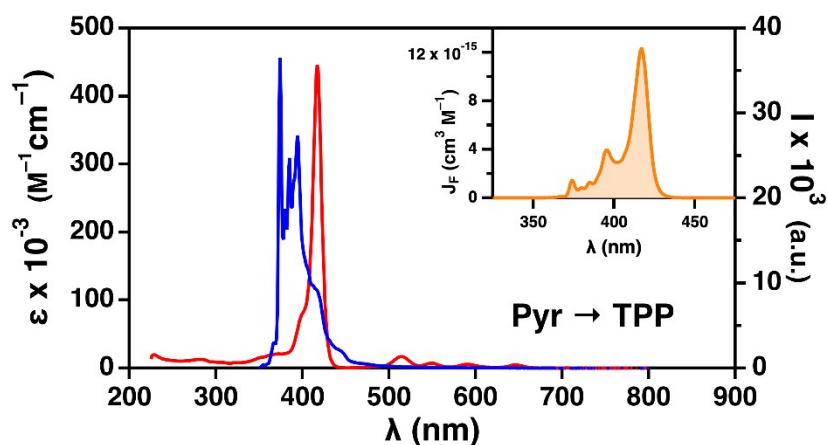


Figure S29. Area normalized emission spectrum of the **Pyr** donor (blue) and the absorption coefficient spectrum of the **TPP** acceptor (red); spectral overlap (inset).

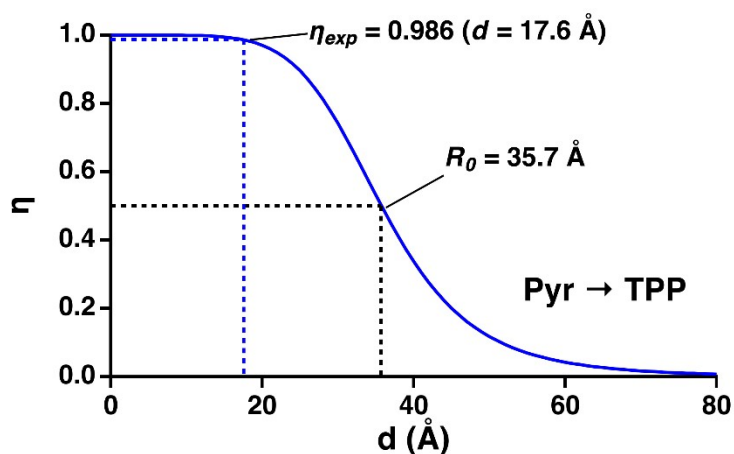


Figure S30. Efficiency of the **Pyr** to **TPP** energy transfer process calculated according to the Förster model ( $\kappa^2 = 2/3$ ).

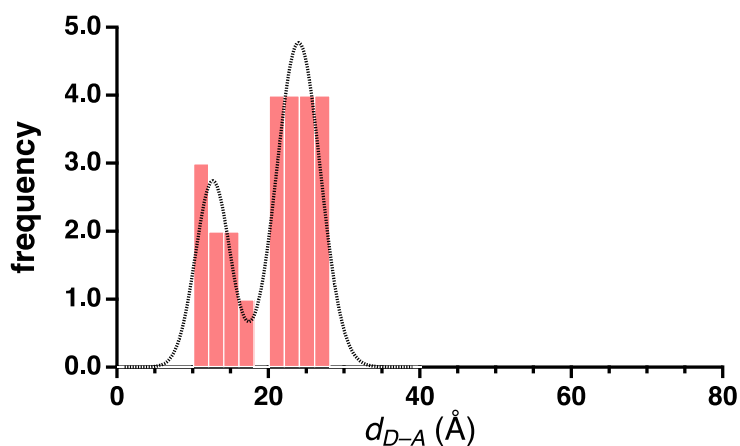


Figure S31. Distribution of the distances between the center of the pyrenyl moieties and the center of the  $N_4$  porphyrin ring in the **P-Pyr<sub>4</sub>@(Rucage)<sub>4</sub>** system, calculated from the molecular modeling (Table S3); the black dotted line is the gaussian interpolation of the distribution.

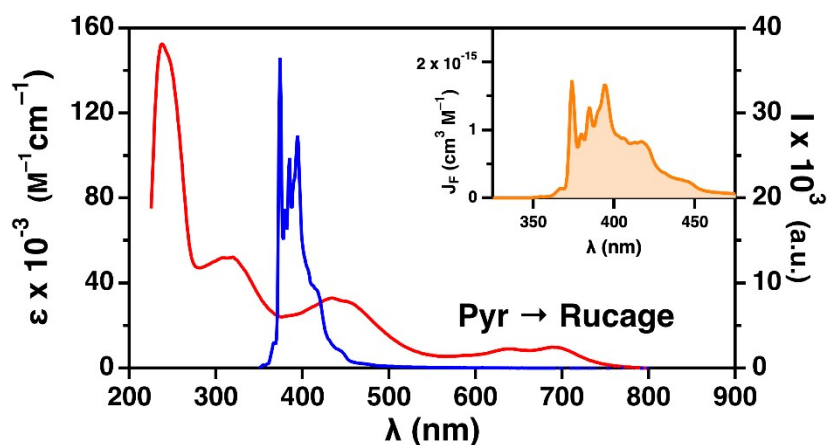


Figure S32. Area normalized emission spectrum of the **Pyr** donor (blue) and absorption coefficient spectrum of the **Rucage** acceptor (red); spectral overlap (inset).

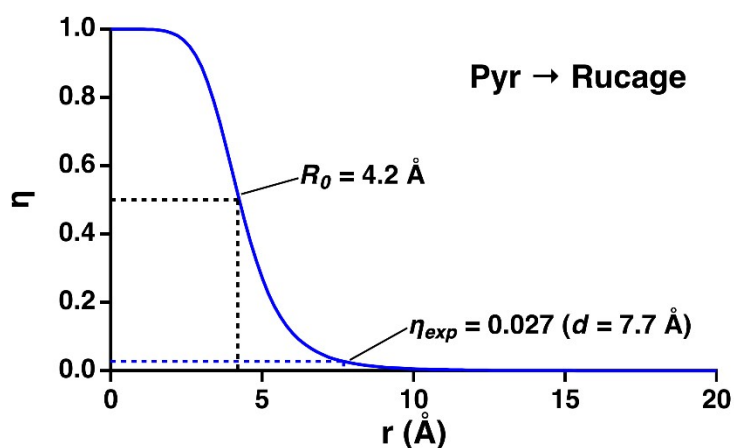


Figure S33. Efficiency of the **Pyr** to **Rucage** energy transfer process calculated according to the Förster model ( $\kappa^2 \sim 0$ ).

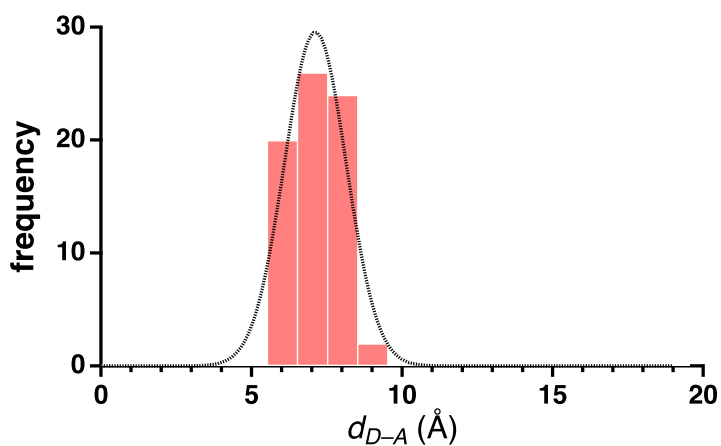


Figure S34. Distribution of the distances between the center of the pyrenyl moieties and the center of the naphthoquinonato pillars in the **P-Pyr<sub>4</sub>@(Rucage)<sub>4</sub>** system, calculated from the molecular modeling (Table S4); the black dotted line is the gaussian interpolation of the distribution.

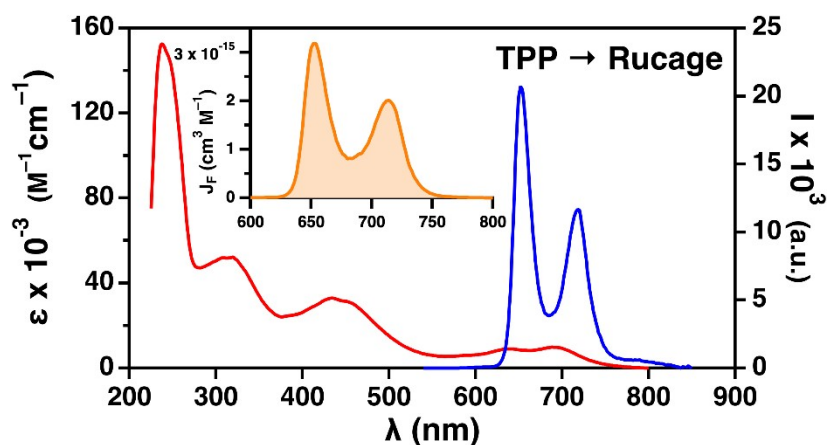


Figure S35. Area normalized emission spectrum of the **TPP** donor (blue) and the absorption coefficient spectrum of the **Rucage** acceptor (red); spectral overlap (inset).

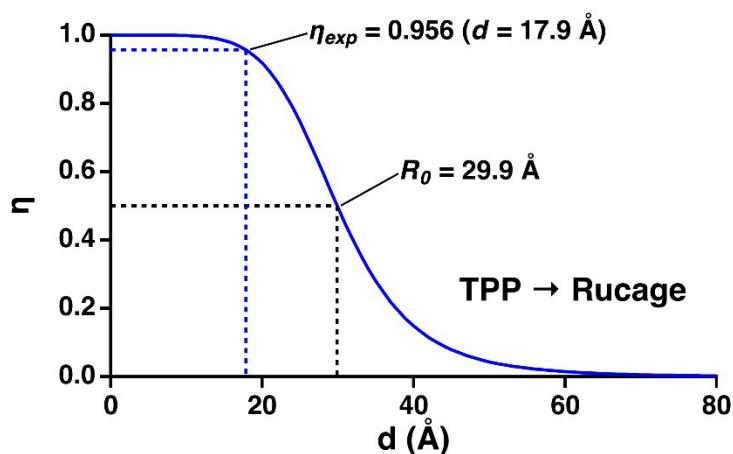


Figure S36. Efficiency of the **TPP** to **Rucage** energy transfer process calculated according to the Förster model ( $\kappa^2 = 2 / 3$ ).

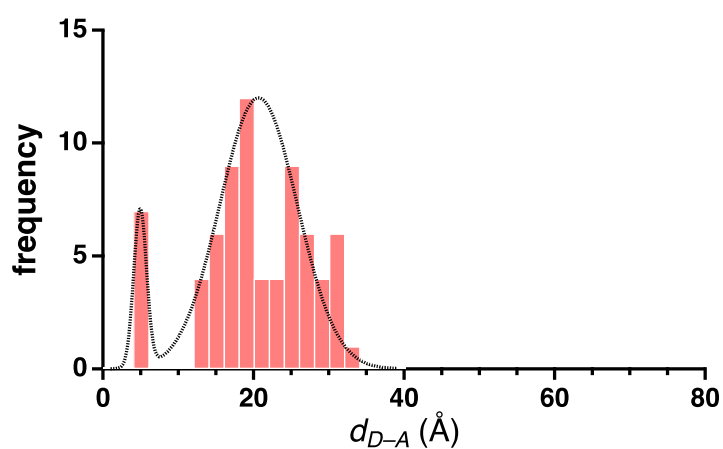


Figure S37. Distribution of the distances between the center of the  $N_4$  porphyrin ring and the center of the naphthoquinonato pillars in the **P-Pyr<sub>4</sub>@(Rucage)<sub>4</sub>** system, calculated from the molecular modeling (Table S5); the black dotted line is the gaussian interpolation of the distribution.

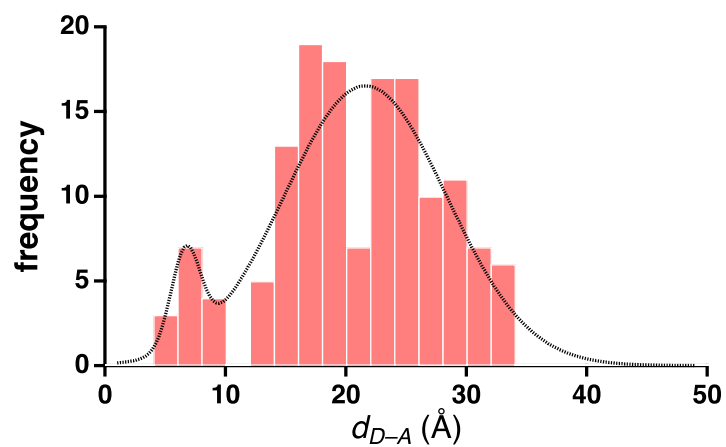


Figure S38. Distribution of the distances between the center of the  $N_4$  porphyrin ring and the ruthenium atoms in the **P-Pyr<sub>4</sub>@(Ru<sub>2</sub>ca<sub>2</sub>)<sub>4</sub>** system, calculated from the molecular modeling (Table S6); the black dotted line is the gaussian interpolation of the distribution.